Radiometric Calibration of Active 3D Imaging Setups Using Superquadric Fitting

James Taylor, Jiazhang Wang, and Florian Willomitzer

Wyant College of Optical Sciences, University of Arizona, Tucson, AZ, USA

ABSTRACT

We present a novel approach for the radiometric calibration of phase-measuring 3D sensors. By combining the projector and camera "nonlinear gamma" parameters into a single total nonlinear factor, we can interpret the global phase error of a radiometrically uncalibrated system as the distortion of a unit circle into a superquadric. Our iterative approach corrects the measurement frames (and therefore the phase errors) by recovering the unit circle of the "undistorted" sinusoidal pattern. In this contribution, we extend this principle of "circularizing" to more complex scenes with varying reflectance.

Keywords: Radiometric calibration, fringe projection, nonlinear gamma

1. INTRODUCTION

Fringe projection profilometry is a well-studied and popular structured light 3D imaging technique. By projecting a sequence of temporally phase shifted sinusoidal intensity patterns[1] onto a scene, a high-resolution 3D measurement can be obtained. Projecting gray scale fringes, however, has a caveat: when any gray scale (or color) image is projected, the projector modifies the input gray values according to its own "emission gamma curve," and when the camera captures the resulting pattern, the final image is altered according to the camera's unique "sensitivity gamma curve." Both the projector and camera gamma curves are commonly nonlinear. If left uncorrected, these nonlinear effects cause the fringes to deviate from being sinusoidal in the captured image. Since the fringe analysis algorithm requires perfectly sinusoidal profiles, the use of distorted fringes without correction in the measurement frames results in phase errors that lead to "ripple artifacts" in the 3D reconstruction (see Fig. 2(e.) and (f.)). The purpose of radiometric calibration is to compensate for this nonlinear distortion by correcting the sinusoidal patterns to recover the true phase. A variety of radiometric calibration techniques have proven effective in correcting this nonlinear intensity transformation. Some methods involve pre-adjusting the pixel intensity of the projected patterns based on a previously calculated nonlinear gamma curve.[2] Others perform a correction after the measurement image is taken, using previously calculated projector-camera response functions[3] or phase look-up tables.[4] While effective, all these methods require the collection of a large set of images from an elaborate separate calibration routine *before* any 3D measurement can be taken. In many cases, this needs to be repeated whenever the setup is changed.

In this contribution, we introduce a novel "on-the-fly" radiometric calibration procedure that does not require a previous calibration session and solely exploits information from the fringe images taken for the actual 3D measurement. As our method does neither rely on prior information about the object nor on information about the scene or setup, it can also be used to calibrate and correct previously captured or old datasets. Our approach assumes the imaging model shown in Fig. 1, which illustrates how the ideal pattern I (computer output to projector) is distorted in the final measurement result, by becoming subject to projector and camera gamma distortions p, c, and varying surface reflectance R (see Fig. 1 (a)-(d)). One of the key observations of this work is that this distortion in the final camera images can be interpreted geometrically through Lissajous figure analysis.[5] Lissajous plotting has been previously used to model and compensate for fringe errors in polarization-based interferometry,[6] using an ellipse-to-circle algorithm. The same principle can be applied for fringe projection. More concrete: the Lissajou plots of perfect sinusoids will be a unit circle. This fact allows us to correct the measured frames using an iterative process, where no prior calibration routine or knowledge about the setup is required. Furthermore, this "on-the-fly" calibration can be adapted to more complex scenes, where scene points with differing reluctance are corrected using distinct Lissajous plots.

Further author information: (Send correspondence to James Taylor and Florian Willomitzer)
E-mail: jrt4@arizona.edu, fwillomitzer@arizona.edu

Interferometry and Structured Light 2024, edited by Michael B. North-Morris, Katherine Creath, Song Zhang, Proc. of SPIE Vol. 13135, 131350E
 · 0277-786X · doi: 10.1117/12.3027875

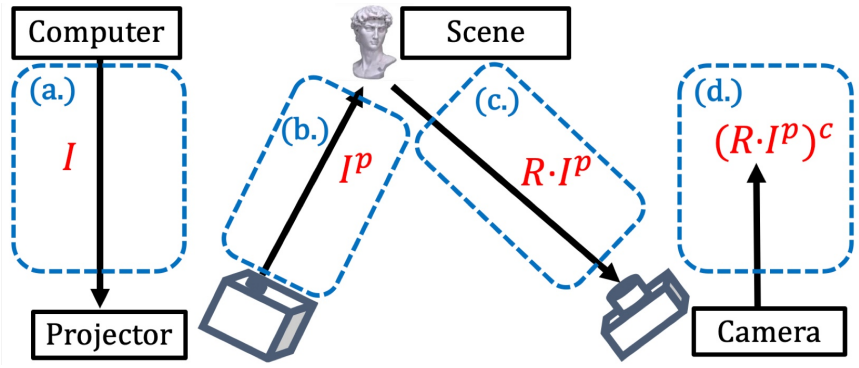

Figure 1. **Our Radiometric Imaging Model for Phase Measuring Triangulation** (a.) A computer transmits the signal of the correct pattern image I to the projector. (b.) The projector then displays a distorted image according to the projector's nonlinear gamma parameter, p. (c.) When the light reflects off the scene, the local surface reflectance applies a multiplicative factor R to the light as it arrives at the camera. (d.) The camera then applies its own nonlinear factor, c to obtain the final output image.

2. METHODS AND RESULTS

Although not limited to a specific number of phase shifts, we demonstrate our method at the example of the well-know "4-phase shift" projection[1] . As explained in,[5] the intensity recorded at each camera pixel (x, y) for the n^{th} phase shift can be described as:

$$I_n(x,y) \quad = \quad [R(x,y)[A + Bsin\{\phi(x,y) + \frac{n\pi}{2}\}]^p]^c, \qquad n = [0,3]. \tag{1}$$

$R(x, y)$ is the surface reflectance, A is the global projector intensity offset, B is the amplitude of the sinusoidal modulation, and p and c denote the projector and camera nonlinear responses, respectively. In this contribution, we assume light from other sources (background illumination, interreflections, etc.) as being negligible by measuring geometrically simple shaped objects in a dark room. In absence of a radiometric calibration, the 4-phase-shift algorithm delivers an incorrect phase result $\phi_{wrong}(x, y)$ through the following equation:

$$\phi_{wrong}(x,y) = arctan(\frac{I_1 - I_3}{I_2 - I_4}) = arctan(\frac{R^c[A + Bsin(\phi(x,y))]^g - R^c[A - Bsin(\phi(x,y))]^g}{R^c[A + Bcos(\phi(x,y))]^g - R^c[A - Bcos(\phi(x,y))]^g}), \qquad g = p \cdot c \tag{2}$$

where $\phi(x, y)$ is the true phase we want to obtain at the location (x,y). In our previous work,[5] we explored the more simple case where the object's reflectance is uniform, i.e., $R(x, y)$ is a constant for all locations (x,y). Under this assumption, we can simply plot the denominator and numerator of the *arctan* argument as a two dimensional graph (denominator: x-value; numerator: y-value). If all captured points in the image accommodate at least one full fringe period, we generate a full sampling of a Lissajou curve (see Fig. 2(c.) and (d.) and reference[5] for details). If no radiometric distortion is present ($p = c = 1$) it can be seen from Eq. 2 that the resulting Lissajou plot is a unit circle. As there is only one combined exponential parameter $g = p \cdot c$, we can solve for the total nonlinear distortion in the system using an iterative procedure that selects the best estimate for g such that when the inverse g^{-1} is applied to the four measurement frames, the resulting Lissajou curve best approximates a unit circle. We direct the reader to reference[5] for details.

Building on our the previous "circularization" approach for uniform reflectance, we herein introduce a method that adapts to *spatially varying reflectance* $R(x, y)$. We start by averaging the four measurement frames $\bar{I} = \sum_{n=0}^{3} I_n/4$ (Fig. 2a), before segmenting the resulting image into multiple regions of different intensity. Each region is identified using binning and thresholding techniques based on the obtained intensity distribution (Fig. 2b). Once segmented, we obtain a unique Lissajou curve for each unique region. We then perform the same iterative process of choosing a g estimate, but optimize under the condition that g must have the same value for all regions in the image. We do this by obtaining a mean squared error (MSE) between each region's Lissajou

plot and their corresponding best fit circle. Summing each region's MSE gives us the metric for determining the accuracy of the chosen g estimate. In this contribution, we assume the best estimate for g to be the one that minimizes this total MSE value. To demonstrate the effectiveness of this expanded circularization technique, we conducte an experiment using a flat landscape photo as the measurement object. As shown in Fig. 2(a.), the average of the four measurement frames was calculated, providing an approximate relative reflectance map. Next, we applied a segmentation and thresholding procedure to divide the image into regions of similar reflectance, as illustrated in Fig. 2(b.). Once segmented, each region's Lissajou figure was plotted and collectively circularized (see Fig. 2(c.) and (d.)), leading to one value for the total system "gamma" across all the regions of different reflectance. The effectiveness of the circularization is highlighted in Fig. 2(e.) and Fig. 2(f.), which present depth profiles taken from two different reflectance regions along lines (I) and (II) shown in Fig. 2(b). Figures 2(e.) and 2(f.) plot the two contour line profiles before and after our "on-the-fly" correction. The results clearly show a significant reduction in the ripple amplitude after "circularization", validating the robustness of our approach for regions with varying reflectance and complex surface geometries.

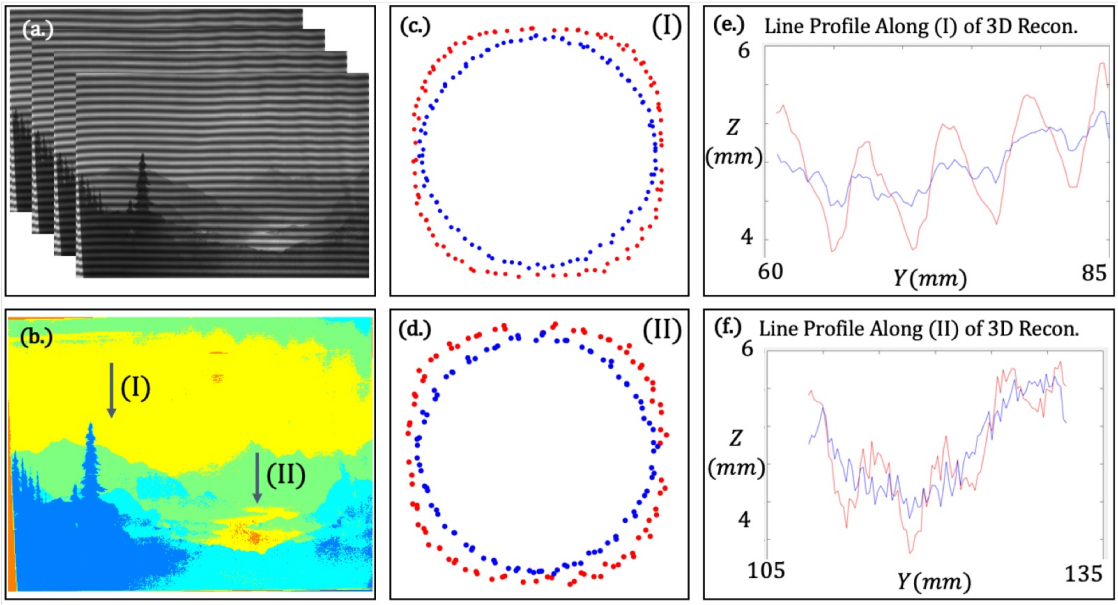

Figure 2. **Results for scene with varying reflectance** (a.) Stack of four measurement frames used to calculate average intensity. (b.) Segmented regions of the image after applying thresholding techniques to identify areas of similar reflectance. (c.)-(f.)In red: Uncalibrated case. In blue: After our circularization correction. (c.) Lissajou plots for points along line (I) for both the uncalibrated case and after circularization. (d.) Lissajou plots for points along line (II) for both the uncalibrated case and after circularization. (e) YZ-line profile of the 3D reconstruction corresponding to the line (I) from (b), showing the ripple artifacts before and after the circularization process. (f.) YZ-line profile of the 3D reconstruction corresponding to the line (II) from (b), showing the ripple artifacts before and after the circularization process.

3. SUMMARY

We have presented a geometric optimization procedure to correct for the nonlinear radiometric system distortion commonly found in fringe projection profilometry and other structured light techniques. Our novel procedure corrects the fringe measurements "on-the-fly," meaning it only uses the information from the measurement frames itself to compensate for the combined camera and projector distortion. We have expanded upon our previously introduced iterative approach of "circularizing" a Lissajou figure for scenes with constant reflectance.[5] With the addition of a segmentation operation, we can account for both a spatially varying reflectance map and a total nonlinear gamma distortion. However, our approach still has limitations, as some of our model assumptions might not be generalizable to the measurement of more complex scenes. Novel optimization-based and deep-learning-based techniques to overcome these limitations are current work in progress.

Acknowledgement: This research was supported by the National Science Foundation under Grant number CMMI-2216298.

REFERENCES

[1] Srinivasan, V., Liu, H. C., and Halioua, M., "Automated phase-measuring profilometry of 3-d diffuse objects," *Appl. Opt.* **23**, 3105–3108 (Sep 1984).

[2] Zhang, X., Zhu, L., Li, Y., and Tu, D., "Generic nonsinusoidal fringe model and gamma calibration in phase measuring profilometry," *J. Opt. Soc. Am. A* **29**, 1047–1058 (Jun 2012).

[3] Debevec, P. E. and Malik, J., "Recovering high dynamic range radiance maps from photographs," in [*Proceedings of the 24th Annual Conference on Computer Graphics and Interactive Techniques*], *SIGGRAPH '97*, 369–378, ACM Press/Addison-Wesley Publishing Co., USA (1997).

[4] Hoang, T., Pan, B., Nguyen, D., and Wang, Z., "Generic gamma correction for accuracy enhancement in fringe-projection profilometry," *Opt. Lett.* **35**, 1992–1994 (Jun 2010).

[5] Taylor, J. R., Wang, J., and Willomitzer, F., ""on-the-fly" radiometric calibration of active 3d imaging setups using superellipse fitting," in [*Frontiers in Optics + Laser Science 2023 (FiO, LS)*], *Frontiers in Optics + Laser Science 2023 (FiO, LS)* , FTu6D.3, Optica Publishing Group (2023).

[6] Kimbrough, B., "Correction of errors in polarization based dynamic phase shifting interferometers," *International Journal of Optomechatronics* **8**(4), 304–312 (2014).